Heat And Mass Transfer On MHD Convective Flow Of Micropolar Fluid Past An Infinite Vertical Porous Surface

N Ravi Kumar[1] & R Bhuvana Vijaya[2]

[1]*Research Scholar ,Department of Mathematics, JNTUA, Anantapuram, AP,India.*
Email: ravinandyala@gmail.com
[2]*Department of Mathematics, JNTUA, Anantapuram, AP,India.*
Email: bhuvanarachamalla@gmail.com

Abstract: We have studied the effects of heat and mass transfer on free convective flow of micro-polar fluid over an infinite vertical porous plate in the presence of an inclined magnetic field with an angle of inclination α with a constant suction. The dimensionless governing equations are reduced to a system of linear differential equations making use of regular perturbation method. The control of various parameters on the flow has been discussed graphically. The temperature increase with increasing heat radiation parameter and reduces with suction parameter. The rate of heat transfer increase with Prandtl number and the rate of mass transfer enhance with chemical reaction parameter.

Keywords: *Convection, Heat transfer, MHD flows, micro-polar fluids, porous media.*

1. INTRODUCTION

Micropolar fluids has many practical applications, for examples analyzing the behavior of exotic lubricants, the flow of colloidal suspensions or polymeric fluids, liquid crystals, additive suspensions, animal blood, body fluids, and turbulent shear flows. Many investigators have studied and reported results for micropolar fluids in external flows [1, 2]. The theory of micro-polar fluids was developed by Eringen [3, 4]. The comprehensive literature on micro-polar fluids, thermo-micro-polar fluids and their applications in engineering and technology were presented by [5, 6]. Srinivasacharya et al. [7] analyzed the unsteady stokes flow of micro-polar fluid between two parallel porous plates. Muthuraj and Srinivas [8] investigated fully developed MHD flow of a micro-polar and viscous fluid in a vertical porous space using HAM. The pioneering works [9, 10] have laid the foundation stone in this field. Many authors have studied the flow and heat transfer in a rotating system with various geometrical situations [11–15]. Veera Krishna et al. [16] discussed heat and mass transfer on unsteady MHD oscillatory flow of blood through porous arteriole. The effects of radiation and Hall current on an unsteady MHD free convective flow in a vertical channel filled with a porous medium have been studied by Veera Krishna et al. [17]. The heat generation/absorption and thermo-diffusion on an unsteady free convective MHD flow of radiating and chemically reactive second grade fluid near an infinite vertical plate through a porous medium and taking the Hall current into account have been studied by Veera Krishna and Chamkha [18]. Veera Krishna and others [21-29] investigated MHD flows through porous media in different configurations. Keeping the above mentioned facts, we have studied the effects of heat and mass transfer on free convective flow of micro-polar fluid over an infinite vertical porous plate in the presence of an inclined magnetic field with an angle of inclination α with a constant suction velocity and taking Hall current into account..

2. Formulation And Solution Of The Problem

We consider an unsteady three dimensional free convective flow of micro-polar fluid over an infinite vertical porous plate in the presence of an inclined magnetic field with an angle of inclination α with a constant suction velocity. The flow is assumed to be in the *x*-direction, which is taken along the plate in upward direction, and the *y*-axis is normal to it and the z-axis along the width of the plate as shown in Fig.1.

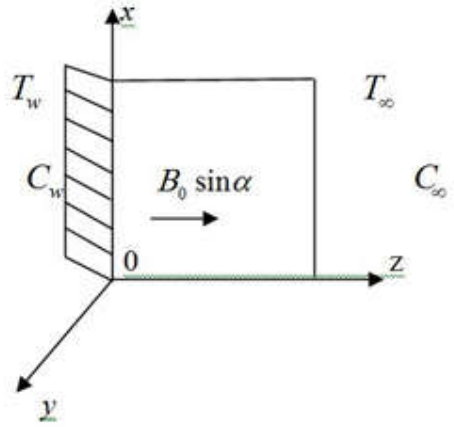

Fig.1 Physical model

The equations for governing flow are:

$$\frac{\partial w}{\partial z} = 0 \tag{1}$$

$$\frac{\partial u}{\partial t} + w\frac{\partial u}{\partial z} = (\nu + \nu_r)\frac{\partial^2 u}{\partial z^2} - \nu_r \frac{\partial N_2}{\partial z} + \frac{\sigma \mu_e^2 H_0^2 \sin^2 \alpha}{\rho} - \frac{\nu}{k}u + g\beta_T (T - T_\infty) + g\beta_C (\mathrm{C} - C_\infty) \tag{2}$$

$$\frac{\partial v}{\partial t} + w\frac{\partial v}{\partial z} = (\nu + \nu_r)\frac{\partial^2 v}{\partial z^2} - \nu_r \frac{\partial N_1}{\partial z} - \frac{\sigma \mu_e^2 H_0^2 \sin^2 \alpha}{\rho} - \frac{\nu}{k}v \tag{3}$$

$$\frac{\partial N_1}{\partial t} + w\frac{\partial N_1}{\partial z} = \frac{\Lambda}{\rho j}\frac{\partial^2 N_1}{\partial z^2} \tag{4}$$

$$\frac{\partial N_2}{\partial t} + w\frac{\partial N_2}{\partial z} = \frac{\Lambda}{\rho j}\frac{\partial^2 N_2}{\partial z^2} \tag{5}$$

$$\frac{\partial T}{\partial t} + w\frac{\partial T}{\partial z} = \frac{k_1}{\rho C_p}\frac{\partial^2 T}{\partial z^2} - \frac{Q}{\rho C_p}(T - T_\infty) + \frac{Q_1^*}{\rho C_p}(\mathrm{C} - C_\infty) - \frac{1}{\rho C_p}\frac{\partial q_r}{\partial z} \tag{6}$$

$$\frac{\partial C}{\partial t} + w\frac{\partial C}{\partial z} = D_m \frac{\partial^2 C}{\partial z^2} - R_r(\mathrm{C} - C_\infty) \tag{7}$$

The relevant boundary conditions are:

$$u=v=0,\ N_1=N_2=0,\ T=T_\infty,\ C=C_\infty \ \text{for}\ \ t\le 0 \tag{8}$$

$$u=U_r\left\{1+\frac{\varepsilon}{2}\left(e^{int}+e^{-int}\right)\right\}, v=0$$

$$N_1=-\frac{1}{2}\frac{\partial v}{\partial z},\ \ N_2=\frac{1}{2}\frac{\partial u}{\partial z},\ \ T=T_w,\ \ C=C_w, \text{ at } z=0,\ \text{for } t>0 \tag{9}$$

$$u=v=0,\ N_1=N_2=0,\ T=T_\infty, C=C_\infty \ \text{ as }\ z\to\infty \tag{10}$$

The oscillatory plate velocity assumed in equation (14) is based on the suggestion proposed by Ganapathy [20]. We now consider a convenient solution of the continuity equation (6) to be

$$v=-v_0 \tag{11}$$

Where, v_0 represents the normal velocity at the plate, which is positive for suction and negative for blowing. The radiative heat flux term by using the Rosseland approximation is given by

$$q_r=-\frac{4\sigma^*}{3k^*}\frac{\partial T^4}{\partial z} \tag{12}$$

$$T^4=4TT^3{}_\infty-3T^4{}_\infty \tag{13}$$

$$\frac{\partial q_r}{\partial z}=-\frac{16T^3{}_\infty\sigma^*}{3k^*}\frac{\partial^2 T}{\partial z^2} \tag{14}$$

Let us introduced the following non-dimensional quantities:

$$u^*=\frac{u}{U},\ v^*=\frac{v}{U_{r,}},\ z^*=\frac{zU_r}{\nu},\ t^*=\frac{tU^2{}_r}{\nu},\ n^*=\frac{n\nu}{U_r^2},\ Q_1=\frac{Q_1^*\left(C_w-C_\infty\right)}{\left(T_w-T_\infty\right)U_r^2}$$

$$N_1^*=\frac{N_1\nu}{U_r^2},\ N_2^*=\frac{N_2\nu}{U_r^2},\ \mathrm{Kc}=\frac{R_r\nu}{U_r^2},\ \ M=\frac{\mu_e H_0}{U_r}\sqrt{\frac{\sigma\nu}{\rho}},\ L=\frac{\Lambda}{\mu j},\ \Delta=\frac{\nu_r}{\nu},\ K=\frac{kU_r^2}{\nu^2}$$

$$F=\frac{4T_\infty^3\sigma}{k_1k^*},\ \ S=\frac{w_0}{U_r},\ \ \mathrm{Sc}=\frac{\nu}{D_m},\ \ \mathrm{Pr}=\frac{\mu C_p}{k},$$

$$\theta=\frac{T-T_\infty}{T_w-T_\infty},\ \phi=\frac{C-C_\infty}{C_w-C_\infty},\ \mathrm{Gr}=\frac{\nu g\beta_T\left(T_w-T_\infty\right)}{U_r^3}$$

$$\mathrm{Gm}=\frac{\nu g\beta_T\left(C_w-C_\infty\right)}{U_r^3},\ Q^*=\frac{Q\nu^2}{U_r^2k}$$

In view of equation (14), the basic field equations (2) - (7) can be expressed in non-

dimensional for as:

$$\frac{\partial u}{\partial t}-S\frac{\partial u}{\partial z}=(1+\Delta)\frac{\partial^2 u}{\partial z^2}-\Delta\frac{\partial N_2}{\partial z}-\left(M^2\sin^2\alpha+\frac{1}{K}\right)u+\left(M^2\sin^2\alpha\right)v+\mathrm{Gr}\theta+\mathrm{Gm}\phi \tag{15}$$

$$\frac{\partial v}{\partial t}-S\frac{\partial v}{\partial z}=(1+\Delta)\frac{\partial^2 v}{\partial z^2}+\Delta\frac{\partial N_1}{\partial z}-\left(M^2\sin^2\alpha+\frac{1}{K}\right)v\ -\left(M^2\sin^2\alpha\right)u \tag{16}$$

$$\frac{\partial N_1}{\partial t}-S\frac{\partial N_1}{\partial t}=L\frac{\partial^2 N_1}{\partial z^2} \tag{17}$$

$$\frac{\partial N_2}{\partial t}-S\frac{\partial N_2}{\partial t}=L\frac{\partial^2 N_2}{\partial z^2} \tag{18}$$

$$\frac{\partial \theta}{\partial t}-S\frac{\partial \theta}{\partial z}=\frac{1}{\mathrm{Pr}}\left(1+\frac{4F}{3}\right)\frac{\partial^2\theta}{\partial z^2}-\frac{Q}{\mathrm{Pr}}\theta+Q_1\phi \tag{19}$$

$$\frac{\partial \phi}{\partial t}-S\frac{\partial \phi}{\partial z}=\frac{1}{\mathrm{Sc}}\frac{\partial^2\phi}{\partial z^2}-\mathrm{Kc}\phi \tag{20}$$

The corresponding boundary conditions are

$$u=v=0,\ N_1=N_2=0,\ \theta_0=0,\phi_0=0\ \text{ for }\ t\le 0 \tag{21}$$

$$u=1+\frac{\varepsilon}{2}\left(e^{int}+e^{-int}\right),\ v=0,\ u=v=0,\ N_1=N_2=0,\ \theta=0,\ \phi=0,\ \text{as}\ z\to\infty \tag{22}$$

To obtain desired solutions, we now simplify equations (15) - (20) by putting the fluid velocity and angular velocity in the complex form as:

$V=u+iv$ and $\omega=N_1+iN_2$ we get

$$\frac{\partial V}{\partial t}-S\frac{\partial V}{\partial z}=(1+\Delta)\frac{\partial^2 V}{\partial z^2}+i\Delta\frac{\partial \omega}{\partial z}-\left(M^2\sin^2\alpha+\frac{1}{K}\right)V-i\left(M^2\sin^2\alpha\right)V+\mathrm{Gr}\theta+\mathrm{Gm}\phi \tag{23}$$

$$\frac{\partial \omega}{\partial t}-S\frac{\partial \omega}{\partial z}=L\frac{\partial^2\omega}{\partial z^2} \tag{24}$$

The associated boundary condition become

$$V=0,\omega=0,\ \theta=0,\phi=0\quad \text{for}\quad t\le 0 \tag{25}$$

$$V=1+\frac{\varepsilon}{2}(e^{int}+e^{-int}),\ \omega=\frac{i}{2}\frac{\partial V}{\partial z},\ \theta=1,\ \phi=1\ \text{at}\ z=0,$$

$$V=0,\omega=0,\theta=0,\ \phi=0,\ \text{as}\ z\to\infty,\ for\ t>0 \tag{26}$$

In order to reduce the above system of partial differential equations in dimensionless form, we may represent the linear and angular velocities, temperature and concentration as V,ω,θ and ϕ as

$$\left.\begin{aligned} V(\mathrm{z,t})=V_0+\frac{\varepsilon}{2}\left\{e^{\mathrm{int}}V_1(z)+e^{-\mathrm{int}}V_2(z)\right\},\omega(z,t)=\omega_0+\frac{\varepsilon}{2}\left\{e^{int}\omega_1(z)+e^{-int}\omega_2(z)\right\}\\ \theta(z,t)=\theta_0+\frac{\varepsilon}{2}\left\{e^{int}\theta_1(z)+e^{-int}\theta_2(z)\right\},\phi(z,t)=\phi_0+\frac{\varepsilon}{2}\left\{e^{int}\phi_1(z)+e^{-int}\phi_2(z)\right\} \end{aligned}\right\} \tag{27}$$

Substituting the above equations (27) into the equations (19), (20), (23) and (24) and equating the harmonic and non-harmonic terms and neglecting the higher order terms $O(\varepsilon^2)$, we obtain the following set of equations

Zeroth order:

$$(1+\Delta)V_0''+SV_0'-a_1V_0+\mathrm{Gr}\theta_0+\mathrm{Gm}\phi_0+i\Delta\omega_0'=0 \tag{28}$$

$$L\omega_0''+S\omega_0'=0 \tag{29}$$

$$(3+4F)\theta_0''+3S\,\mathrm{Pr}\,\theta_0'-3Q\theta_0+3Q_1\,\mathrm{Pr}\,\phi_0=0 \tag{30}$$

$$\phi_0''+S\mathrm{Sc}\phi_0'-\mathrm{KcSc}\phi_0=0 \tag{31}$$

First order

$$(1+\Delta)V_1''+SV_1'-a_2V_1+\mathrm{Gr}\theta_1+\mathrm{Gm}\phi_1+i\Delta\omega_1'=0 \tag{32}$$

$$L\omega_1''+S\omega_1'-in\omega_1=0 \tag{33}$$

$$(3+4F)\theta_1''+3S\,\mathrm{Pr}\,\theta_1'-3(Q+in\,\mathrm{Pr})\theta_1+3Q_1\,\mathrm{Pr}\,\phi_1=0 \tag{34}$$

$$\phi_1''+S\mathrm{Sc}\phi_1'-(\mathrm{Kc}+in)\phi_1=0 \tag{35}$$

Second order equations are:

$$(1+\Delta)V_2''+SV_2'-a_3V_2+\mathrm{Gr}\theta_2+\mathrm{Gm}\phi_2+i\Delta\omega_2'=0 \tag{36}$$

$$L\omega_2''+S\omega_2'+in\omega_2=0 \tag{37}$$

$$(3+4\mathrm{F})\theta_2''+3S\,\mathrm{Pr}\,\theta_2'-3(Q-in\,\mathrm{Pr})\theta_2+3Q_1\,\mathrm{Pr}\,\phi_2=0 \tag{38}$$

$$\phi_2''+S\mathrm{Sc}\phi_2'-(\mathrm{Kc}-in)\phi_2=0 \tag{39}$$

Where, the prime denote differentiation with respect to z

The corresponding boundary conditions can be written as

$$V_0=V_1=V_2=1,\omega_0=\frac{i}{2}V_0',\omega_1=\frac{i}{2}V_1',\ \omega_2=\frac{i}{2}V_1'$$

$$\theta_0 = 1, \theta_1 = \theta_2 = 0, \phi_0 = 1, \phi_1 = \phi_2 = 0, \quad \text{at} \quad z = 0 \tag{40}$$

$$V_0 = V_1 = V_2 = 0, \omega_0 = \omega_1 = \omega_2 = 0$$

$$\theta_0 = 1,\ \theta_1 = \theta_2 = 0,\ \phi_0 = 1,\ \phi_1 = \phi_2 = 0, \text{ at } z \to \infty \tag{41}$$

Solving equation (28) - (38) under the boundary conditions (40) & (41) we obtain the expressions for translation velocity, micro-rotation, temperature and concentrations as:

$$V = A_3 e^{-m_1 z} + A_4 e^{-m_2 z} + A_5 e^{-m_3 z} + A_6 e^{-(S/L)z} + \frac{\varepsilon}{2}\left\{\left(A_7 e^{-m_4 z} + A_8 e^{-m_5 z}\right)e^{int} + \left(A_8 e^{-m_6 z} + A_{10} e^{-m_7 z}\right)e^{int}\right\} \tag{42}$$

$$\omega = B_1 e^{-(S/L)z} + \frac{\varepsilon}{2}\left\{B_2 e^{int - m_4 z} + B_3 e^{-int + m_6 z}\right\} \tag{43}$$

$$\theta = A_1 e^{-m_1 z} + A_2 e^{-m_2 z} \tag{44}$$

$$\phi = e^{-m_1 z} \tag{45}$$

The physical quantities of engineering interest are skin friction coefficient, couple stress coefficient number and Sherwood number. The Skin friction is caused by viscous drag in the boundary layer around the plate, and then it is important to discuss the skin friction from the knowledge of velocity, free skin friction non-dimensional form can be calculated as follows:

$$C_f = \frac{\tau_{\omega|z=0}}{\rho U_r^2} = \left\{1 + \Delta\left(1 + \frac{i}{2}\right)\right\} V'(0)$$

$$= -\left\{1 + \Delta\left(1 + \frac{i}{2}\right)\right\}\left[A_3 m_1 + A_4 m_2 + A_5 m_3 + \frac{S}{L}A_6 + \frac{\varepsilon}{2}\left\{\left(A_7 m_4 + A_8 m_5\right)e^{int} + \left(A_9 m_6 + A_{10} m_7\right)e^{int}\right\}\right] \tag{46}$$

The couple stress coefficient at the wall C_s is given by

$$C_s = \left.\frac{\partial \omega_1}{\partial z}\right|_{z=0} + i\left.\frac{\partial \omega_2}{\partial z}\right|_{z=0} = \omega'(0)$$

$$= -\left\{\frac{SB_1}{L} + \frac{\varepsilon}{2}\left(B_2 m_4 e^{int} + B_3 m_6 e^{-int}\right)\right\} \tag{47}$$

The rate of heat transfer between the fluid and the plate is studied through non-dimensional Nusselt number. The rate of heat transfer in terms of Nusselt number is given by

$$N_u = \frac{\chi\left(\frac{\partial T}{\partial z}\right)_{z=0}}{T_w - T_\infty} = -\mathrm{Re}_x\,\theta'(0) \Rightarrow \frac{N_u}{\mathrm{Re}_x} = -\theta'(0)$$

$$= A_1 m_1 + A_2 m_2 \qquad (48)$$

Where, $\mathrm{Re}_x = \frac{U_r x}{\nu}$ is the local Reynolds number

The local Sherwood number Sh_x is given by

$$Sh_x = -\frac{\chi\left(\frac{\partial C}{\partial z}\right)_{z=0}}{C_w - C_\infty} = -\mathrm{Re}_x\,\phi'(0)$$

$$\Rightarrow \frac{Sh_x}{\mathrm{Re}_x} = -\phi'(0) = m_1 \qquad (49)$$

3. Results And Discussion

The Figs. 2 represent the primary and secondary velocity profiles for different values of a magnetic field parameter *M*. Both the velocity components decrease with increase in a magnetic field parameter *M* along the surface. The reversal behavior is observed with increasing the permeability parameter *K* (Figs. 3). Here particularly we observed that lower the permeability lesser the fluid speed in the entire fluid region. Again from the figures (4 & 5), we noticed that both the velocity components enhance with increasing heat radiation parameter *F* and additional heat source *Q*. Finally the velocity components *u* and *w* decrease with increasing the angle of inclination α (Figs. 6).

The micro-rotation profiles for N_1 are negative because the micro-rotation of the fluid is anti-clockwise. Figs. (7) depict the micro-rotational velocity profiles for N_1 and N_2 with different values of magnetic field parameter *M*. The micro-rotational velocity distribution for N_1 increase and N_2 are decrease with an increase in the magnetic field parameter (Hartmann number) throughout the fluid region. The effects due to permeability of the porous parameter (*K*) on micro-rotational velocity are shown in Figs. (8). It is observed that as the permeability parameter increases, the micro-rotational velocity components N_1 decrease and N_2 increase in entire flow field. We also observed that the velocity component N_1 reduce and N_2 increase with increasing heat radiation parameter *F* and additional heat source *Q*. This has been seen from Figures (9 - 10). From

the Figs. (11), we found that the velocity component N_1 increase and N_2 decrease with increasing angle of inclination α. We also distinguished that from the Figs. (30) an increase in Schmidt number Sc leads to reduce temperature. It is observed that from the Fig. (12), temperature is boost up with increasing heat radiation parameter *F* in the entire flow region. Fig. (13) evident that, the influence of suction parameter S.. The Figs. (14-15) exhibits the resultant concentration with respect to the governing parameters Sc and Kc, and is reduces with increasing Sc and *K*c.

Table 1 shows that the skin friction C_f and couple stress coefficient C_s both are upsurges with increasing heat radiation parameter *F,* Grashof number Gr, frequency of oscillation *n.* The skin friction C_f and couple stress coefficient C_s both are reduce with increasing magnetic field parameter *M,* Pr Prandtl number. We also noticed that an increase in mass Grashof number Gm and viscosity ratio Δ, the skin friction C_f is increase and the couple stress coefficient C_s is decrease. It is observed from the table 1. the skin friction C_f is decrease and the couple stress coefficient C_s is increase while increase in permeability parameter *K*, Schmidt number Sc, suction parameter *S* and chemical reaction parameter *K*c Table 2 illustrates how the rate of heat transfer from the walls to the fluid is influenced by governing parameters Pr, *Q*, *F*, Sc, α and Q_1. It is observed that the surface heat transfer decreases with the increasing values of Prandtl number Pr, additional heat source parameter *Q*, heat radiation parameter *F*, and radiation absorption parameter Q_1 and also amplified with increasing in suction parameter *S*, Schmidt number Sc and chemical reaction parameter *K*c.

Velocity profile

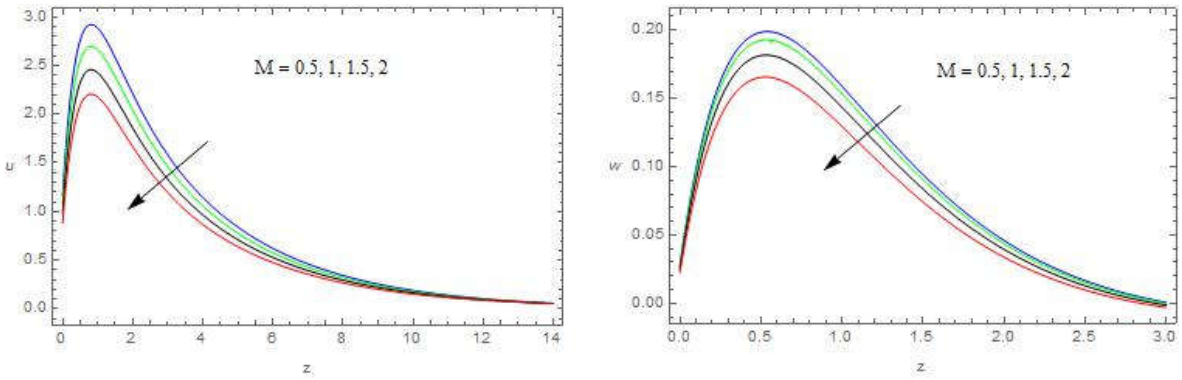

Figs. 2 The velocity profiles against *M* with
$K = 0.5, \Pr = 0.71, \alpha = \pi/6, \mathrm{Kc} = 1, \mathrm{Gr} = 3, \mathrm{Gm} = 2, \mathrm{Sc} = 0.22, n = \pi/6, \Delta = 0.1, S = 1, F = 0.2, Q = 1, Q_1 = 0.2$

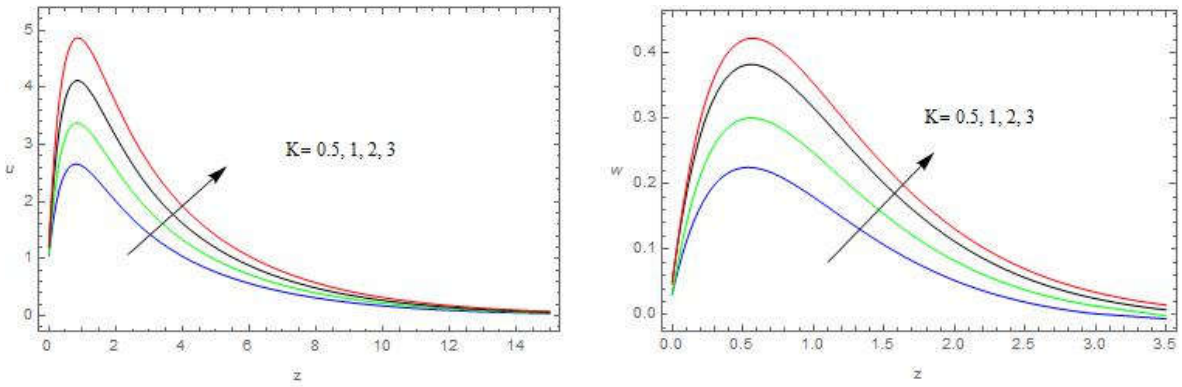

Figs. 3 The velocity profiles against K with

$M = 0.5, \Pr = 0.71, \alpha = \pi/6, \mathrm{Kc} = 1, \mathrm{Gr} = 3, \mathrm{Gm} = 2, \mathrm{Sc} = 0.22, n = \pi/6, \Delta = 0.1, S = 1, F = 0.2, Q = 1, Q_1 = 0.2$

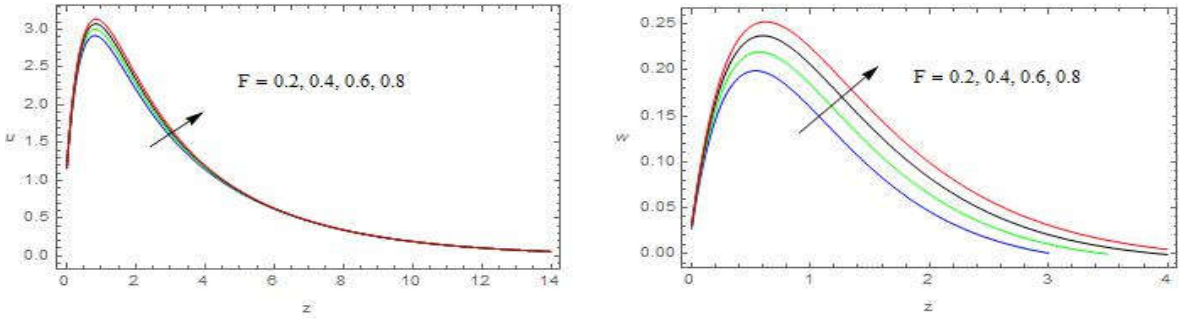

Figs. 4 The velocity profiles against F with

$M = 0.5, K = 0.5, \Pr = 0.71, \alpha = \pi/6, \mathrm{Kc} = 1, \mathrm{Gr} = 3, \mathrm{Gm} = 2, \mathrm{Sc} = 0.22, n = \pi/6, \Delta = 0.1, S = 1, Q = 1, Q_1 = 0.2$

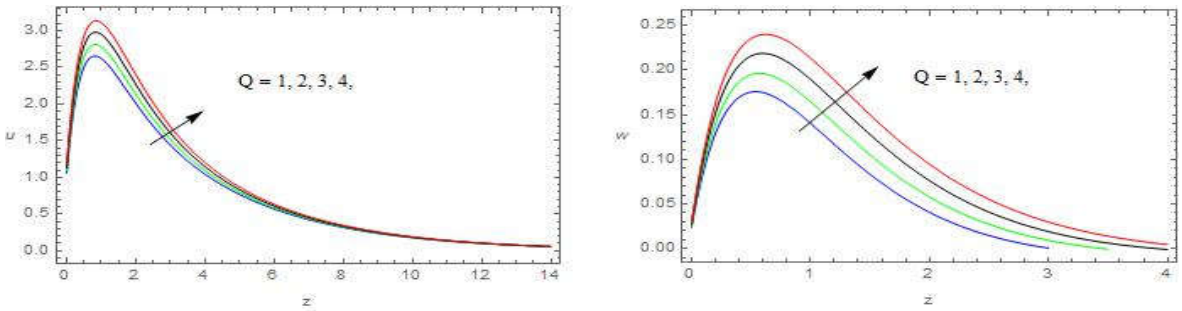

Figs 5.The velocity profiles against Q with

$M = 0.5, K = 0.5, \Pr = 0.71, \alpha = \pi/6, \mathrm{Kc} = 1, \mathrm{Gr} = 3, \mathrm{Gm} = 2, \mathrm{Sc} = 0.22, n = \pi/6, \Delta = 0.1, S = 1, F = 0.2, Q_1 = 0.2$

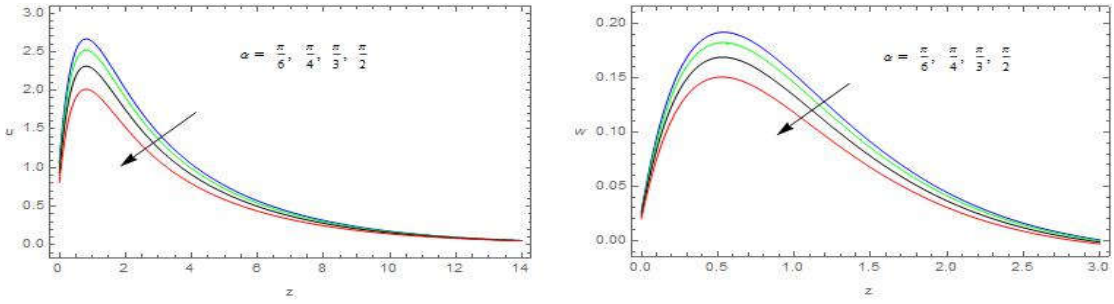

Figs. 6 The velocity profiles against α with

$M = 0.5, K = 0.5, \Pr = 0.71, \mathrm{Kc} = 1, \mathrm{Gr} = 3, \mathrm{Gm} = 2, \mathrm{Sc} = 0.22, n = \pi/6, \Delta = 0.1, S = 1, F = 0.2, Q = 1, Q_1 = 0.2$

Micro rotation profile

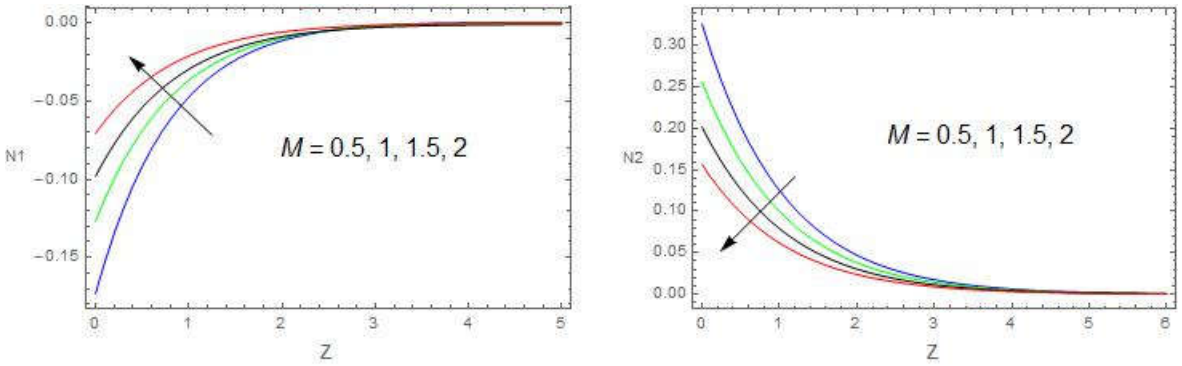

Figs. 7 The Micro rotation profiles against M with

$K = 0.5, \Pr = 0.71, \alpha = \pi/6, \mathrm{Kc} = 1, \mathrm{Gr} = 3, \mathrm{Gm} = 2, \mathrm{Sc} = 0.22, n = \pi/6, \Delta = 0.1, S = 1, F = 0.2, Q = 1, Q_1 = 0.2$

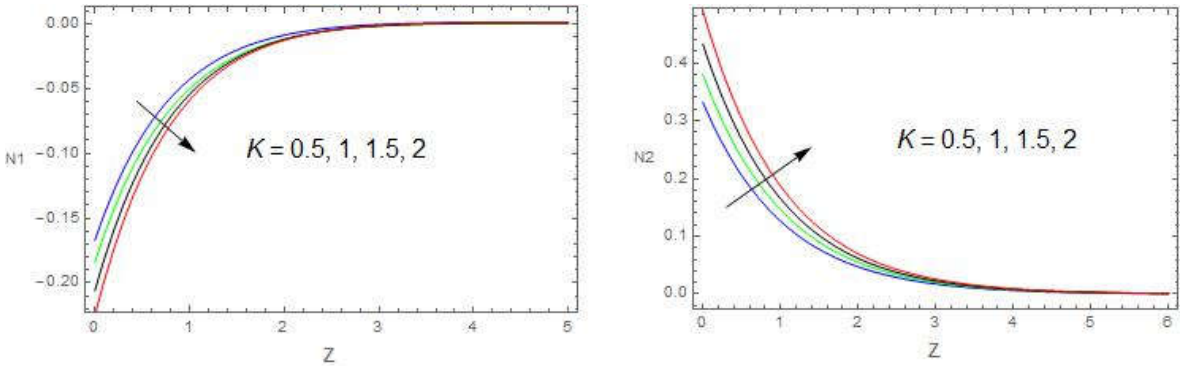

Figs 8. The Micro rotation profiles against K with

$M = 0.5, \Pr = 0.71, \alpha = \pi/6, \mathrm{Kc} = 1, \mathrm{Gr} = 3, \mathrm{Gm} = 2, \mathrm{Sc} = 0.22, n = \pi/6, \Delta = 0.1, S = 1, F = 0.2, Q = 1, Q_1 = 0.2$

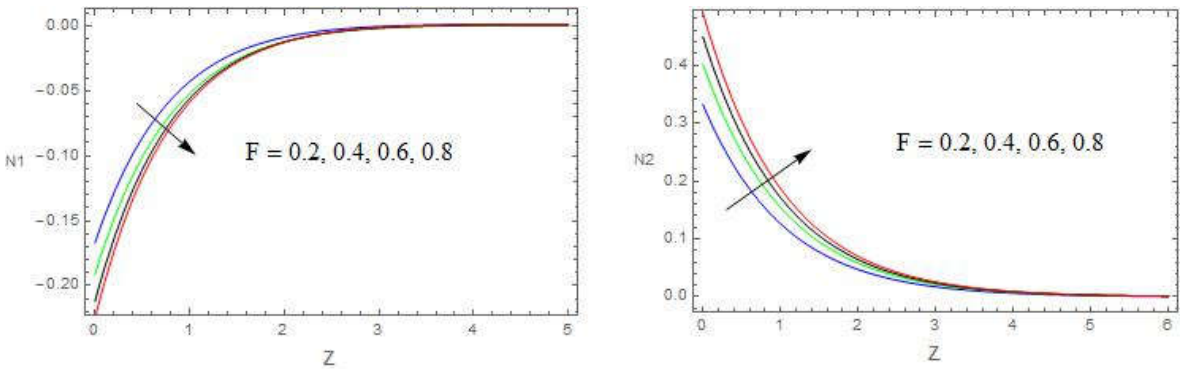

Figs 9.The Micro rotation profiles against F with

$M=0.5, K=0.5, \Pr=0.71, \alpha=\pi/6, \mathrm{Kc}=1, \mathrm{Gr}=3, \mathrm{Gm}=2, \mathrm{Sc}=0.22, n=\pi/6, \Delta=0.1, S=1, Q=1, Q_1=0.2$

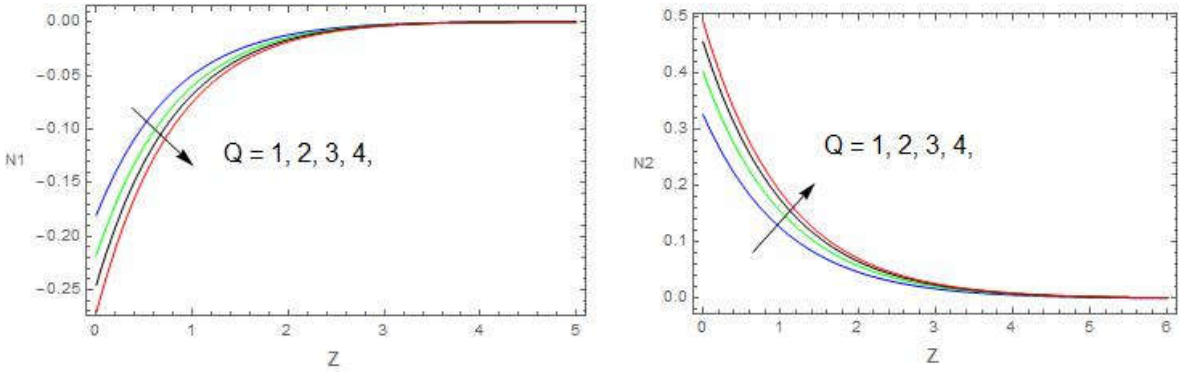

Figs 10.The Micro rotation profiles against Q with

$M=0.5, K=0.5, \Pr=0.71, \alpha=\pi/6, \mathrm{Kc}=1, \mathrm{Gr}=3, \mathrm{Gm}=2, \mathrm{Sc}=0.22, n=\pi/6, \Delta=0.1, S=1, F=0.2, Q_1=0.2$

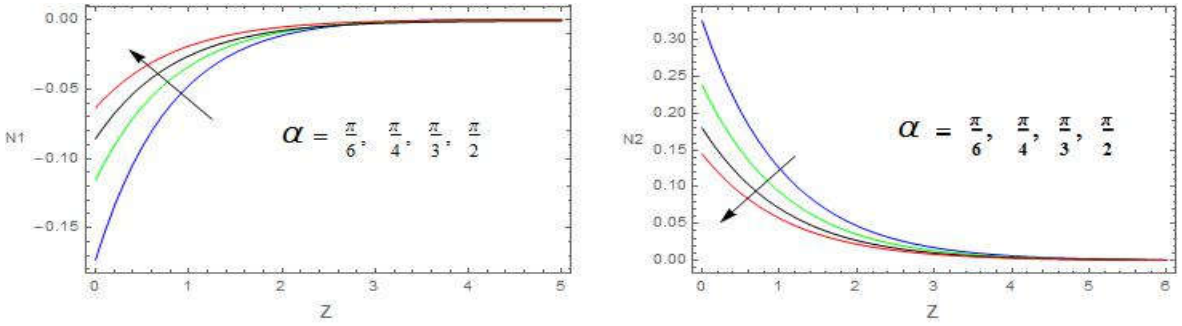

Figs 11.The Micro rotation profiles against with α

$M=0.5, K=0.5, \Pr=0.71, \mathrm{Kc}=1, \mathrm{Gr}=3, \mathrm{Gm}=2, \mathrm{Sc}=0.22, n=\pi/6, \Delta=0.1, S=1, F=0.2, Q=1, Q_1=0.2$

Temperature Profiles

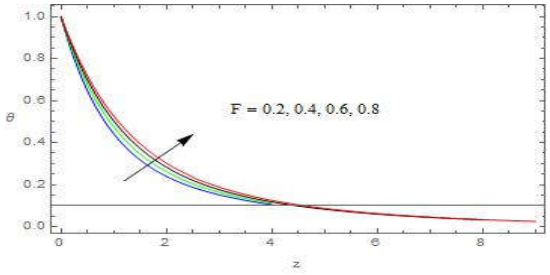

Figs 12.The Temperature profiles against F with

$\mathrm{Sc}=0.22, S=1, Q_1=1, Kc=1$

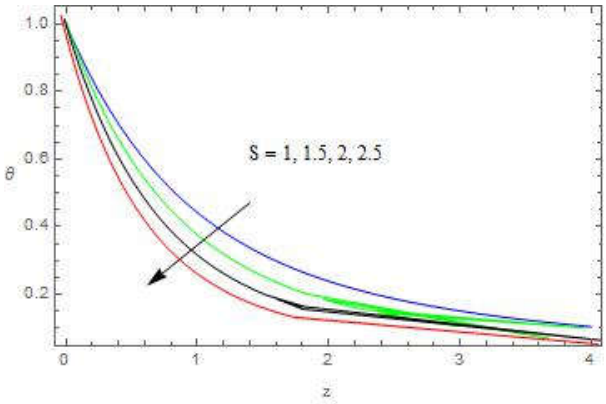

Figs 13.The Temperature profiles against S with $\mathrm{Sc}=0.22, Q_1=1, F=0.2, Kc=1$

Concentration Profiles

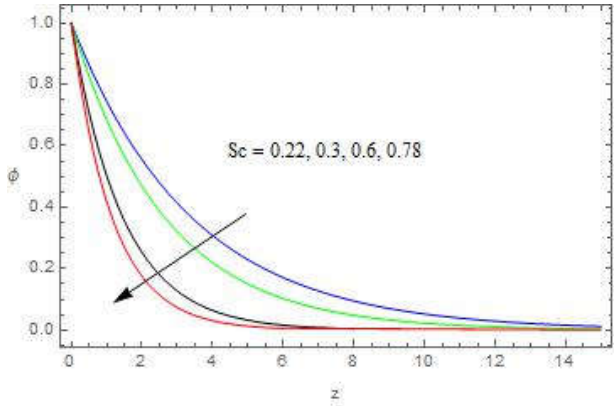

Figs. 14 The Concentration profiles against Sc with $S=1, Kc=1$

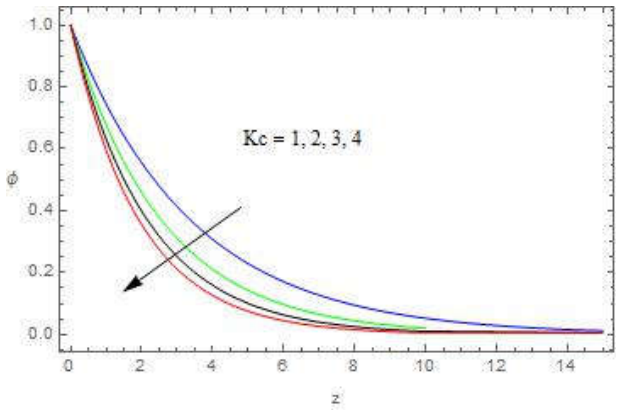

Figs 15.The Concentration profiles against *K*c with $\mathrm{Sc}=0.22, S=1,$

Table 1: Frictional force and Couple stress co-efficient

Pr	M	F	Sc	α	K	S	n	Δ	Gr	Gm	C_f	C_s
0.71	0.5	0.2	0.22	0.1	0.5	1	$\pi/6$	0.1	3	2	7.72785	0.959356
3											6.39336	0.705325
7											5.47588	0.493985
	1										7.59140	0.962879
	1.5										7.71778	0.968999
		0.4									7.89856	0.996251
		0.6									8.09245	1.025000
			0.3								7.34999	0.977525
			0.6								6.32621	1.002456
				0.3							7.27656	0.987785
				0.5							7.10989	1.014115
					1						6.35889	1.085748
					2						5.73998	1.154965
						1.5					7.40325	1.497777
						2					7.04969	2.095658
							$\pi/4$				8.18958	1.120748
							$\pi/3$				7.98958	1.282145
								0.2			9.75777	0.913333
								0.3			10.1362	0.872998
									4		10.5898	1.386978
									5		13.2445	1.814528
										3	8.57996	0.876555
										4	9.01845	0.793898

Table2: Nusselt number

S	Pr	Q	F	Sc	α	Q_1	Nu
0	0.71	1	0.2	0.22	0.1	0.5	0.618220
1							0.915702
2							1.323740
	3						-0.253603
	6						-1.395730
		2					-0.429284
		3					0.135285
			0.4				0.565369
			0.6				0.522467
				0.3			0.624555
				0.6			0.641263
					0.3		0.643843
					0.5		0.658834
						1	0.347917
						1.5	0.077613

Table 3: Sherwood number

Sc	S	α	Sh_x
0.22	1	0.1	0.294662
0.3			0.379129
0.6			0.687298
	3		0.48533
	2		0.691801
		0.3	0.389464
		0.5	0.459428

Table 4: Comparison of results

$\Pr = 0.71, \alpha = 0.1, \mathrm{Gr} = 3, \mathrm{Gm} = 2, \mathrm{Sc} = 0.22, n = \pi/6, \Delta = 0.1, S = 1, F = 0.2, Q = 1$

$\varepsilon = 0.01, t = 1, z = 0.5$

M	K	Previous Results Das [19] for velocity u	Present results $Q_1=0$ for velocity u	Previous Results Das [19] for micro-rotational velocity N_1	Present results $Q_1=0$ for micro-rotational velocity N_1
0.5	0.5	2.75120	2.75118	-0.0640853	-0.0640841
1		2.74854	2.74851	-0.0640141	-0.0640098
1.5		2.73493	2.73488	-0.0638959	-0.0638899
2		2.72830	2.72826	-0.0637317	-0.0637288
	1	2.86682	2.86678	-0.0772872	-0.0772788
	2	3.48735	3.48731	-0.0894623	-0.0894597
	3	3.99979	3.99975	-0.0955901	-0.0955874

Table 3 shows that the effect of Sc, S, and α on Sherwood number sh_x. The rate of mass transfer increase with increasing all parameters Schmidt number Sc or suction parameter S and/or chemical reaction parameter Kc. To verify the validity and accuracy of the present analysis, our results have been compared to the velocity and micro-rotation velocity with Das [19]. The results of this comparison are given in Table 4. It can be seen from this table that excellent agreement between the results exists. In addition, we observed that the fluid velocity and micro-rotations are lower for polar fluids than for Newtonian fluids.

4. Conclusions

The velocity reduces with increasing Hartmann number, where as it enhance with Q. The micro-rotational velocity increases with increasing K. The temperature increase

with increasing heat radiation parameter and reduces with suction parameter. Concentration reduces with increasing chemical reaction parameter. The magnitude of skin friction at the plate is found to decrease due to increasing the Hartmann number *M* and frequency of oscillation and increase with heat radiation parameter *F*. The magnitude of couple stress coefficient increases with Kc and reduces with Gm. The rate of heat transfer increase due to increase in *S* reduces with Pr. The rate of mass transfer enhance with Sc, *S* and Kc.

References:

[1]. Bhargava R, Anwar Beg O, Sharma S, Zueco J. Finite element study of nonlinear two-dimensional deoxygenated bio-magnetic micro-polar flow. Commun Nonlinear Sci Numer Simul 2010; 15:1210–23.

[2]. Sarifuddin, Chakravarty Santabrata, Mandal Prashanta Kumar. Heat transfer to micropolar fluid flowing through an irregular arterial constriction. Int J Heat Mass Transfer 2013;56:538–51.

[3]. Eringen AC. Simple micro fluids. Int J Eng Sci 1964;2:205–17.

[4]. Eringen AC. Theory of thermomicrofluids. J Math Anal Appl1972;38:480–96.

[5]. Ariman T, Turk MA, Sylvester ND. Micro-continuum fluid mechanics-a review. Int J EngSci 1973;11:905–30.

[6]. Prathap Kumar J, Umavathi JC, Chamkha Ali J, Pop I. Fully developed free convective flow of micro-polar and viscous fluids in a vertical channel. Appl Math Model 2010;34:1175–86.

[7]. Srinivasacharya D, Ramanamurthy JV, Venugopalam D. Unsteady stokes flow of micro-polar fluid between two parallel porous plates. Int J Eng Sci 2001;39:1557–63.

[8]. Muthuraj R, Srinivas S. Fully developed MHD flow of a micro-polar and viscous fluids in a vertical porous space using HAM. Int J Appl Math Mech 2010;6(11):55–78.

[9]. Hickman KCD. Centrifugal boiler compression still. Ind Eng Chem 1957;49:786–800.

[10]. Mazumder BS. An exact solution of oscillatory Couette flow in a rotating system. ASME J Appl Mech 1991;58(4):1104–7.

[11]. Ezzat MA, Mohamed IA, Othman, Helmy KA. A problem of a micro-polar magneto-hydrodynamic boundary layer flow. Can J Phys 1999;77:813–27.

[12]. Chakraborti A, Gupta AS, Das BK, Jana RN. Hydromagnetic flow past a rotating porous plate in a conducting fluid rotating about a non-coincident parallel axis. ActaMech2005;176:107–19.

[13]. Ezzat MA, Mohamed IA, Othman. Thermal instability in a rotating micro-polar fluid layer subject to an electric field. Int J Eng Sci 2000;38:1851–67.

[14]. Mohamed IA, Othman, Zaki SA. Thermal relaxation effect on magneto-hydro-dynamic instability in a rotating micropolar fluid layer heated from below. Acta Mech. 2004; 170(1-4):187–97.

[15]. Mohamed IA, Othman, Zaki SA. Thermal instability in a rotating micropolar viscoelastic fluid layer under the effect of electric field. Mech Mech Eng 2008; 12(2):171–84.